Separation Science and Technology
Publication details, including instructions for authors and subscription information:
http://www.informaworld.com/smpp/title~content=t713708471

QSPR Modelling of Lanthanide-Organic Complex Stability Constants

Ruslan Svetlitski[a]; Andre Lomaka[b]; Mati Karelson[b]
[a] Department of Chemistry, University of Tartu, Tartu, Estonia [b] Department of Chemistry, Tallinn University of Technology, Tallinn, Estonia

To cite this Article Svetlitski, Ruslan , Lomaka, Andre and Karelson, Mati(2006) 'QSPR Modelling of Lanthanide-Organic Complex Stability Constants', Separation Science and Technology, 41: 1, 197 — 216
To link to this Article: DOI: 10.1080/01496390500446194
URL: http://dx.doi.org/10.1080/01496390500446194

Separation Science and Technology, 41: 197–216, 2006

ISSN 0149-6395 print/1520-5754 online
DOI: 10.1080/01496390500446194

QSPR Modelling of Lanthanide-Organic Complex Stability Constants

Ruslan Svetlitski
Department of Chemistry, University of Tartu, Tartu, Estonia

Andre Lomaka and Mati Karelson
Department of Chemistry, Tallinn University of Technology, Tallinn, Estonia

Abstract: The quantitative structure–property relationships (QSPR) have been developed for the stability constants of complexes between 63 different organic ligands and 14 lanthanides. The QSPR models for a series involving a single metal were constructed using only theoretical descriptors for ligands within the CODESSA program. The QSPR models for the series of constants with constant ligand were constructed using various physical properties of metals as descriptors. A good quality of models (47 of the 63 models for ligands gave R^2 higher than 0.90 and only 6 had $R^2 < 0.80$ and 10 of the 14 models for metals gave R^2 higher than 0.87 and no model had $R^2 < 0.84$) enables reliable prediction of stability constants for any previously unmeasured complex.

Keywords: QSPR, lanthanide, complex, stability constant, molecular descriptors

INTRODUCTION

There is considerable interest in the syntheses, structure, and luminescence and magnetic resonance spectral properties of novel binuclear compounds exhibiting electronic lanthanide (III)–lanthanide (III) (Ln^{3+}–Ln^{3+}) coupling (1–6). For instance, the potential for such couplings to produce

Received 7 October 2005, Accepted 30 October 2005
Address correspondence to Andre Lomaka, Department of Chemistry, Tallinn University of Technology, Akadeemia tee 15, Tallinn, Estonia. Tel.: + 372 6 202 819; Fax: +372 6 202 819; E-mail: andre.lomaka@ttu.ee

unusual tuneable electronic behavior can be exploited to generate sharper image contrasts in magnetic resonance (MRI) (7, 8) and fluorescence imaging continues to spur interest in these compounds (9, 10). Significant water solubility and stability of some binuclear lanthanide (III) compounds make them also attractive as various biomedical agents. For example, free Gd (III) ion is extremely toxic at the concentrations needed for MRI studies. However, being administered in the form of stable complexes, the metal ion is not released before excretion (11).

The complex stabilities are also very important for the development of new efficient methods of separation of lanthanides from solution. It is well known that the separability depends on the stability constants of the complexes formed (12).

The above-listed applications require the development of lanthanide chelates with carefully tailored chemical, structural and spectroscopic (or magnetic) properties. Thus, the aim of the present work is the development of predictive QSPR models of stability constants for lanthanide complexes with organic ligands. Such models enable to make reliable predictions of the stability constants for previously unknown complexes and to elucidate the structural factors determining the stability of complexes.

DATA SET

The data set of experimental stability constants of complexes between lanthanide ions and structurally variable organic ligands was compiled from the literature (cf. references from Table 1). For the QSPR model development, the logarithmic constants $\log K_1$ were used, where K_1 is defined as follows:

$$K_1 = \frac{[LnL^{n+3}]}{[Ln^{3+}][L^n]}$$

All stability constants correspond to aqueous solutions at the ionic force $\mu = 0.1$ and temperature 25°C.

Table 1 gives the list of the 66 different organic ligands that were selected for the present QSPR study, each with 6 or more data points. Tables 2 and 3 include the additional information about the chemical structure of the organic ligands used. In Table 4, the 23 different metal descriptors that were used in present QSPR study are listed.

METHODOLOGY

The geometrical structure of ligand molecules was optimized using the AM1 (13) method within the MOPAC (14) program package. The geometry and other information from the output of quantum chemical calculations were

Table 1. The organic ligands used in the QSPR treatment

No	Ligand name	Ref.
1	IMDA	I–III
2	Maleic acid	IV
3	Acetate	III
4	α-Hydroxy-isobutyric acid	III
5	4-Aminobenzoate	V
6	4-Hydroxybenzoate	V
7	4-Nitrobenzoate	V
8	Acrylic acid	IV
9	Methacrylic acid	IV
10	K22DAP	VI
11	K22DA	VI
12	K22DP	VI
13	K22MA	VI
14	K21DA	VI
15	EDTA	I, III
16	EDDA	I, III
17	Malonic acid	VII
18	4-dimethylaminobenzylidenepyruvate	VIII
19	4-dimethylaminocinnamylidenepyruvate	VIII
20	Acetylacetone	III
21	1,2-Cyclohexylenedinitrilotetraacetic acid	I, III
22	BENTA	I
23	BIMDA	I
24	DTPA	I
25	EDTP	I, III
26	EEDTA	I, III
27	EGTA	I, IIII
28	HEDTA	I, III
29	MEPDA	I, III
30	MIMDA	I, III
31	Nitrilotriacetic acid	I, III
32	PIMDA	I, III
33	Glycolic acid	IIIX
34	Metoxyacetic acid	III
35	Glyoxalic acid	III
36	a-Hydroxypropionic acid	III
37	Picolinic acid	III
38	Piperidin-2,6 dicarboxy acid	III
39	Glycine	III
40	Trimethylenediaminetetraacetic acid	I, III
41	Triethylenetetraaminehexaacetic acid	I
42	CA	I
43	IDS	I

(*continued*)

Table 1. Continued

No	Ligand name	Ref.
44	BCA	I
45	BCAM	I
46	BCG	I
47	EDDM	I
48	EDDS	I
49	EDDG	I
50	DPDS	I
51	2-OPDTA	I
52	OPDM	I
53	OPDS	I
54	OPDG	I
55	EDDIP	I
56	EDAP	I
57	EDTMP	I
58	OEAIP	I
59	TEAIP	I
60	DETAIP	I
61	OFIDA	I
62	KMIDA	I
63	DGL	I

I. Kostromina, N.A., 1980. Complexing agents of rare earth metals, Nauka, Moscow; II. Hramov, V.P., 1974. Complexing agents of rare earth metals, Saratov university; III. Yatsimirskii, K.B., Kostromina, N.A., Sheka, Z. Davidenko, N. K., Kriss, E.E., Ermolenko, V.I., 1966. Chemistry of Complex Compounds of Rare Earth Elements. Naukova Dumka, Kiev (Russian Edition); IV. Panvushkin, V.T., Achrimenko, N.V., Khachatrian, A.S., 1998. Mixed-ligand complexes of three valent lanthanide ions with acetylacetone and some organic unsaturated acids. Polyhedron. 17, 3053–3058; V. Yun, S.J., Kang, S.K., Yun, S.S., 1999. Thermodynamics of complexation of lanthanides by some benzoic acid derivatives in aqueous solution. Thermochim. Acta. 333, 13–19; VI. Kim, J., Lee, C. N., Han, S. H., Suh, M. Y., 1997. Studies on complexation and solvent extraction of lanthanides in the presence of diaza-18 crown-6-di-isopropionic acid. Talanta, 45, 437–444; VII. Hirikawa, T., Hashimoto, Y., 1997. Simultaneous separation of yttrium and lanthanide ions by isotachophoresis. J. Chromatogr. A 772, 357–367; VIII. Pereira, N.C.S., Melios, C.B., Marques, R.N., Siqueira, O.S., De Morales, M., Molina, M., 1997. 4-Dimethylaminocinnamylidene-pyruvic acid: synthesis, characterization and complexation with trivalent lanthanides, yttrium(III), scandium(III), thorium(IV), and uranium(VI) in aqueous solution. J. Alloys Compd. 297, 94–97;

inserted into the CODESSA (15) program, and descriptors for ligands were calculated. All these descriptors are derived solely from molecular structure and do not require experimental data to be calculated. Various data on physical properties were used as the descriptors for metals (Table 4). The

Table 2. The ligand substructures

1 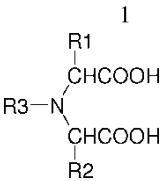	2 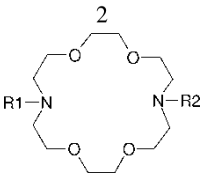	3 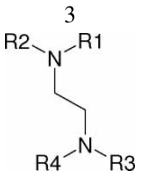	
4 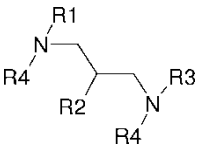	5 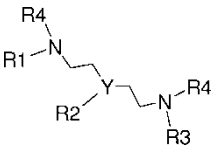	K21DA 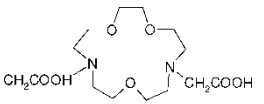	DGL 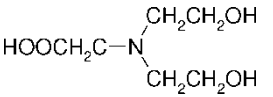

Table 3. The ligand structures

No.	Ligand	R1	R2	R3	R4	Substructure
1	IMDA	–H	–H	–H	—	1
10	K22DAP	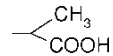	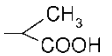	—	—	2
11	K22DA	$-CH_2COOH$	$-CH_2COOH$	—	—	2
12	K22DP	$-CH_2CH_2COOH$	$-CH_2CH_2COOH$	—	—	2
13	K22MA	–H	$-CH_2COOH$	—	—	2
15	EDTA	$-CH_2COOH$	$-CH_2COOH$	$-CH_2COOH$	$-CH_2COOH$	3
16	EDDA	$-CH_2COOH$	–H	$-CH_2COOH$	–H	3
22	BENTA	–H	–H	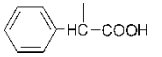	—	1
23	BIMDA	–H	–H	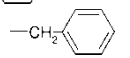		1
24	DTPA	$-CH_2COOH$	$-CH_2COOH$	$-CH_2COOH$	$-CH_2CH_2COOH$	5 (Y=N)
25	EDTP	$-CH_2CH_2COOH$	$-CH_2CH_2COOH$	$-CH_2CH_2COOH$	$-CH_2COOH$	3
26	EEDTA	$-CH_2COOH$	—	$-CH_2COOH$	$-CH_2COOH$	(Y=O)
27	EGTA	$-CH_2COOH$	—	$-CH_2COOH$	$-CH_2CH_2OH$	(Y= OCH_2CH_2O)
28	HEDTA	$-CH_2CH_2OH$	$-CH_2COOH$	$-CH_2COOH$	$-CH_2COOH$	4
29	MEPDA	–H	–H	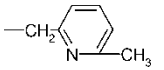	—	1
30	MIMDA	–H	–H	$-CH_3$	—	1
32	PIMDA	–H	–H	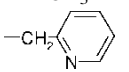	—	1
42	CA	$-CH_2COOH$	–H	–H	—	1
43	IDS	$-CH_2COOH$	$-CH_2COOH$	–H	—	1

44	BCA	–H	–H	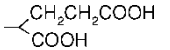	—	1
45	BCAM	–H	–H	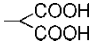	—	1
46	BCG	–H	–H	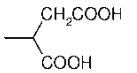	—	1
47	EDDM	–H	–H	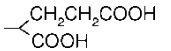	—	3
48	EDDS	–H	–H	$-CH_2COOH$	—	3
49	EDDG	–H	–H	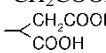	—	3
50	DPDS	$-CH_2COOH$	–H	$-CH_2COOH$	–H	4
51	2-OPDTA	$-CH_2COOH$	–OH	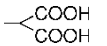	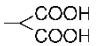	4
52	OPDM	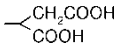	–OH	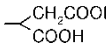	–H	4
53	OPDS	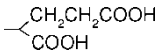	–OH	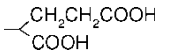	–H	4
54	OPDG		–OH		–H	4
55	EDDIP	$-CH_2PO_3H_2$	–H	$-CH_2COOH$	–H	3
56	EDAP	$-CH_2PO_3H_2$	$-CH_2COOH$	$-CH_2PO_3H_2$	$-CH_2PO_3H_2$	3
57	EDTMP	$-CH_2PO_3H_2$	$-CH_2PO_3H_2$			3
58	OEAIP		—			5 (Y=O)
59	TEAIP		—			5 (Y=S)
60	DETAIP		–H			5 (Y=N)
61	OFIDA	–H	–H	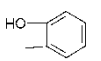		1
62	KMIDA	–H	–H	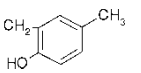		1

Table 4. The external descriptors for lanthanides.

Notation	F01[a]	F02 [b]	F03[c]	F04 [d]	F05[e]	F06[f]	F07[g]	F08[h]	F09[i]	F10[j]	F11[k]	F12[l]
La	538.1	1067	1850.3	4819	0.207	138.906	57	2.74	22.39	3469	373.9	1.69
Ce	534.4	1050	1949	3547	0.209	140.116	58	2.7	20.69	3257	365	1.65
Pr	527	1020	2086	3761	0.21	140.908	59	2.67	20.8	3212	364	1.65
Nd	533.1	1040	2130	3900	0.215	144.24	60	2.64	20.59	3067	362.8	1.64
Sm	544.5	1070	2260	3990	0.224	150.36	62	2.59	19.98	1778	357.9	1.62
Eu	547.1	1085	2404	4120	0.227	151.964	63	2.56	28.97	1597	398.9	1.85
Gd	593.4	1170	1990	4250	0.235	157.25	64	2.54	19.9	3233	357.3	1.61
Tb	565.8	1110	2114	3839	0.237	158.925	65	2.51	19.3	3041	352.5	1.59
Dy	573	1130	2200	3990	0.243	162.5	66	2.49	19.01	2335	350.3	1.59
Ho	581	1140	2204	4100	0.246	164.93	67	2.47	18.74	2720	348.6	1.58
Er	589.3	1150	2194	4120	0.25	167.26	68	2.45	18.46	2510	346.8	1.57
Tm	596.7	1160	2285	4120	0.252	168.934	69	2.42	19.1	1950	344.7	1.56
Yb	603.4	1174.8	2417	4203	0.258	173.04	70	2.4	24.84	1467	388	1.74
Lu	523.5	1340	2022.3	4370	0.261	174.967	71	2.25	17.78	3315	343.5	—

Notation	F13[m]	F14[n]	F15[o]	F16[p]	F17[q]	F18[r]	F19[s]	F20[t]	F21[u]	F22[v]	F23[w]
La	6.146	0.0126	1.1	400	6.2	431	920	117.2	130	26.392	13.5
Ce	6.689	0.0115	1.12	350	5.5	423	795	115	128.3	26.622	11.4
Pr	6.64	0.0148	1.13	356	6.9	330	935	113	126.6	27.195	12.5
Nd	6.8	0.0157	1.14	328	7.1	285	1010	112.3	124.9	27.406	16.5
Sm	7.353	0.00956	1.17	207	8.6	175	1072	109.8	121.9	29.621	13.3
Eu	5.244	0.0112	1.2	175	9.2	175	822	108.9	120.6	27.657	13.9
Gd	7.901	0.00736	1.2	398	10	305	1311	107.8	119.3	37.111	10.6
Tb	8.219	0.00889	1.2	389	10.8	295	1360	106.3	118	28.607	11.1
Dy	8.551	0.0108	1.22	290	11.1	280	1412	105.2	116.7	28.113	10.7

Ho	8.795	0.0124	1.23	301	17	265	1470	104.1	115.5	27.213	16.2
Er	9.066	0.0117	1.24	317	19.9	285	1522	103	114.4	28.1	14.3
Tm	9.321	0.015	1.25	232	16.8	250	1545	102	113.4	27.029	16.8
Yb	6.57	0.0351	1.1	152	7.7	160	824	100.8	112.5	26.821	34.9
Lu	9.841	–	1.27	428	22	–	1656	–	111.7	26.245	16.4

[a]1st ionisation potential, $kJ \cdot mol^{-1}$.
[b]2nd ionisation potential, $kJ \cdot mol^{-1}$.
[c]3rd ionisation potential, $kJ \cdot mol^{-1}$.
[d]4th ionisation potential, $kJ \cdot mol^{-1}$.
[e]Atomic energy, ergs.
[f]Atomic mass.
[g]Atomic number.
[h]Atomic radius, angstrom.
[i]Atomic volume, $cm^3 \cdot mol^{-1}$.
[j]Boiling point, °C.
[k]Bond length in Me - Me, pm.
[l]Bonding radius (covalent radius), angstrom,
[m]Density, $g \cdot cm^{-3}$.
[n]Electrical conductivity, $10^6 \cdot cm^{-1} \cdot Ohm$
[o]Electronegativity.
[p]Enthalpy of atomisation $kJ \cdot mol^{-1}$.
[q]Heat (Enthalpy) of fusion, $kJ \cdot mol^{-1}$.
[r]Heat (Enthalpy) of vaporization, $kJ \cdot mol^{-1}$.
[s]Melting point,^{0}C.
[t]Radius 6-coordinate, octahedral, ion (III), pm.
[u]Radius 8-coordinate, ion (III), pm.
[v]Specific heat, $J \cdot mol^{-1} \cdot K^{-1}$.
[w]Thermal conductivity, $W \cdot m^{-1} \cdot K^{-1}$.

CODESSA program was then used to find the best QSPR multilinear equations with 2, 3, or 4 descriptors depending on the size of the data set for a series of ligand complexes with a given metal. Analogously, the QSPR equations were developed for a series of metal complexes with a given ligand. Both Heuristic and Best Multi-Linear correlation algorithms available in the CODESSA were used. The respective methodology has been described elsewhere (16). The CODESSA program has already been successfully applied to correlate molecular structure with various properties including melting points (17), response factors (15), critical micelle concentrations (18, 19), aqueous solubility of gases (20), glass transition temperatures of polymers (21), and solvent polarity scales (22).

RESULTS AND DISCUSSION

In Tables 5 and 6, the results of the QSPR treatment are summarized for the series of the organic ligands and the lanthanides, respectively. In the first column of Table 5, the ligands are listed in order given in Table 1, and the second column in both Tables 5 and 6 shows the number of experimental data points in the treatment, respectively. The coefficients of QSPR equations and the notations of the respective descriptors are given in the next columns, together with the *t*-test values. The natural value of the regression coefficient itself cannot be treated as an indicator of the importance of the descriptor in an equation as the absolute numeric values of the descriptors vary in a large range. Thus, the *t*-test value for each descriptor has been used instead for the purpose. The last three columns of Tables 5 and 6 show the statistical parameters of the QSPR equations: the squared correlation coefficients (R^2), the squared standard deviation (s^2), and the squared cross-validated correlation coefficients (R^2_{cv}). Most of the developed QSPR equations for ligands have satisfactory correlation coefficient; 47 out of 63 models for ligands have R^2 higher than 0.90 and only 6 models has $R^2 < 0.80$. In the case of QSPR equations for metals, 10 out of 14 models for metal have R^2 higher than 0.87 and no models have $R^2 < 0.84$.

The notations of the descriptors that were used in equations of Table 5 are listed in Table 4. The notations of the descriptors that were used in equations of Table 6 are presented in Table 7. All descriptors from Table 4 are different properties of lanthanides. The descriptors in Table 7 can be divided into six groups. The largest groups include the hydrogen bonding descriptors (6 descriptors), topological indices of the organic ligands (5), general electronic properties (5 descriptors) and bonding interactions (5 descriptors). In addition, descriptors reflecting the geometry and constitution (3) of ligands and partial surface areas (3) did appear in the QSPR models. The hydrogen bonding descriptors were involved 11 times, descriptors describing geometry and constitution of the ligands 10 times, the partial

Table 5. The QSPR models ($a_0 + a_1d_1 + a_2d_2 + a_3d_3 + a_4d_4$) on complex stability constants for organic ligands[a]

Ligand	a_0	n[b]	a_1	d_1	*t*-test	a_2	d_2	*t*-test	a_3	d_3	*t*-test	R^2	s^2	R^2_{cv}
1	21.0	14	−1.01	F15	−2.24	−3.45E-07	F01	−4.15	−0.103	F20	−17.7	0.984	4.28E-03	0.972
2	3.81	13	−1.34E-06	F18	−6.49	3.93-07	F02	1.97	−0.0126	F23	−4.59	0.835	2.52-03	0.508
3	4.02	14	−0.0152	F13	−0.984	−8.79-07	F18	−3.38	−2.75E-06	F01	−3.25	0.711	4.25E-03	0.412
4	−0.911	14	0.0659	F07	24.9	6.28E-08	F04	1.69	6.51	F14	3.67	0.988	1.54E-03	0.963
5	−0.0477	10	9.30E-07	F02	1.33	−4.62E-07	F04	−2.97	0.0249	F21	2.33	0.687	6.45E-03	0.949
6	2.45	10	−5.12	F05	−3.56	−7.89E-07	F18	−3.31	0.621	F15	1.37	0.775	4.07E-03	0.360
7	−3.36	10	−1.96E-06	F01	−2.24	−8.95E-08	F04	−0.761	−6.41E-07	F18	−1.81	0.660	4.58E-03	0.312
8	0.58	9	−6.28E-07	F18	−4.08	−8.07-06	F17	−3.27	0.696	F08	5.26	0.963	5.09E-04	0.886
9	2.56	9	−3.95E-07	F18	−4.09	−5.80E-06	F17	−4.57	−3.92	F14	−5.12	0.904	2.46E-04	0.598
10	16.2	8	−0.121	F23	−6.30	−7.27E-07	F04	−5.08				0.939	1.43E-02	0.815
11	15.2	8	−0.380	F13	−14.4	−1.51E-06	F18	−3.85				0.978	7.06E-03	0.943
12	12.5	8	−6.21E-05	F17	−3.94	−1.21E-06	F04	−4.21				0.871	5.90E-02	0.405
13	8.79	8	−4.12E-06	F18	−5.71	−4.51E-05	F17	−4.45				0.931	2.29E-02	0.791
14	18.2	8	−69.8	F14	−2.57	1.50E-06	F04	4.79				0.883	6.57E-02	0.683
15	−0.645	14	0.298	F07	34.9	−1.96E-07	F04	−1.51				0.991	1.91E-02	0.985
16	18.8	14	−3.64	F08	−15.4	−1.78E-06	F18	−5.06	−2.05E-07	F04	−2.00	0.971	1.14E-02	0.877
17	9.50	14	−3.53E-02	F13	−5.42	−6.94	F14	−6.79	−3.96E-02	F20	−22.3	0.990	3.44E-04	0.978
18	−5.31	14	−0.681	F08	−5.32	−8.54E-07	F18	−4.25	−2.03E-06	F01	−3.03	0.831	3.03E-03	0.647
19	2.78	14	−7.43E-07	F18	−3.15	8.43E-07	F02	3.64	−1.77E-07	F23	−3.02	0.809[c]	3.17E-03	0.937
20	17.8	14	−0.0982	F13	−4.35	−0.0184	F23	−4.60	0.0924	F21	−16.5	0.984	3.75E-03	0.917
21	45.9	13	5.19E-05	F17	4.66	2.61E-02	F23	3.83	−2.59E-01	F20	−21.5	0.997	1.11E-02	0.989
22	15.6	6	−0.236	F12	−6.79	0.0433	F23	1.69				0.948	9.50E-03	0.795
23	21.1	9	−0.0219	F23	−1.27	−0.0385	F11	−9.18				0.933	1.03E-02	0.822

(*continued*)

Table 5. Continued

Ligand	a_0	n[b]	a_1	d_1	*t*-test	a_2	d_2	*t*-test	a_3	d_3	*t*-test	R^2	s^2	R^2_{cv}
24	43.0	14	−5.56E-06	F18	−4.81	−59.1	F14	−3.93	−0.173	F20	−8.73	0.935	0.112	0.873
25	1.82	14	2.95E-01	F07	41.2	−8.70E-07	F16	−2.76	−3.41E-06	F01	−2.83	0.996	8.76E-03	0.990
26	28.1	14	−3.02	F08	−5.37	−6.09E-06	F18	−7.05	−0.594	F23	−4.49	0.894	6.06E-02	0.717
27	36.5	14	−4.13E-05	F17	−3.67	−20.3	F01	−3.32	−1.57E-01	F21	−14.7	0.980	1.46E-02	0.961
28	26.0	14	−3.93	F08	−10.8	−3.18E-06	F18	−5.80				0.945	2.87E-02	0.885
29	20.1	14	−1.40E-07	F04	−2.14	−0.106	F21	−32.6				0.990	4.94E-03	0.953
30	20.5	9	−8.59	F12	−16.8	0.0304	F23	3.23				0.981	3.15E-03	0.946
31	23.2	14	−4.12	F08	−21.0	−1.41E-06	F18	−4.82	−1.97E-07	F04	−2.31	0.982	7.84E-03	0.964
32	19.6	14	−3.62	F08	−20.6	−2.57E-07	F04	−3.31	−1.34E-06	F16	−5.11	0.980	6.64E-03	0.93
33	0.106	14	−5.12E-07	F18	−3.73	2.28	F15	10.5	17.5	F14	9.26	0.952	1.72E-03	0.829
34	2.57	13	−.3.33E-07	F18	−6.48	2.09E-06	F17	2.74	−7.62E-07	F01	−4.59	0.817	1.88E-04	0.662
35	1.08	14	7.24E-07	F02	12.8	3.95E-07	F03	13.6	−0.0107	F09	−6.35	0.979	2.31E-04	0.937
36	1.88	14	−1.30	F08	−11.0	−4.59E-07	F16	−2.56				0.926	3.15E-03	0.890
37	9.53	14	−7.01E-08	F04	−2.54	−0.0471	F20	−27.5	−3.23E-05	F10	−2.46	0.990	8.70E-04	0.960
38	14.1	14	−2.69	F08	−35.8	−2.13E-07	F04	−6.54	−8.53E-07	F18	−7.62	0.993	1.15E-03	0.985
39	15.6	13	−0.128	F13	−5.34	−17.9	F14	−4.85	−0.0983	F20	−15.4	0.977	4.47E-03	0.962
40	−8.46	9	0.357	F07	59.7	−1.39E-07	F04	−1.78				0.998	5.53E-03	0.996
41	227.1	12	−18.3	F07	−2.79	−8.46E-07	F04	−4.97				0.802	2.46E-02	0.702
42	9.22	14	1.04E-03	F19	12.1	31.9	F14	7.95	−1.76E-06	F18	−5.85	0.956	8.55E-03	0.908
43	10.7	14	−6.80E-07	F18	−7.05	1.08	F15	7.07	−4.73	F14	−3.56	0.929	8.51E-04	0.868
44	6.93	14	1.53E-06	F02	3.23	1.24E-06	F03	7.29	4.05E-04	F19	3.27	0.924	0.0101	0.865
45	6.23	14	3.71E-06	F01	3.59	−2.17E-03	F11	−1.46	0.0254	F06	10.2	0.970	6.64E-03	0.947
46	−1.75	14	0.0983	F23	3.22	11.4	F15	12.2	−4.65E-07	F04	−2.77	0.955	0.0312	0.923
47	19.9	14	−2.31	F08	−5.72	−4.17E-06	F18	−6.76	−0.364	F23	−3.85	0.896	0.0309	0.744
48	11.5	14	−4.00E-06	F18	−8.86	−7.59E-07	F04	−5.23	5.59E-06	F02	10.4	0.949	0.0201	0.571

49	26.9	14	−5.80E-07	F16	−1.13	−0.169	F20	−20.2				0.976	2.44E-02	0.959
50	21.9	14	2.96E-04	F19	2.51	7.19E-07	F03	3.71	−1.27E-01	F20	−15.8	0.994	5.22E-03	0.979
51	−16.5	8	0.115	F06	6.34	15.3	F15	3.57				0.936	0.293	0.211
52	5.57	14	0.229	F13	10.0	1.61E-06	F03	8.53				0.938	0.0125	0.902
53	31.3	14	−1.73E-06	F16	−4.67	−0.161	F21	−30.6	−28.5	F14	−5.77	0.991	0.0111	0.983
54	−2.87	14	1.36E-01	F07	15.6	−3.25E-02	F09	−2.57	1.60E-06	F03	6.20	0.988	9.84E-03	0.978
55	226.1	13	−6.38	F08	−6.58	6.04E-05	F10	−3.31	6.79E-06	F01	1.44	0.913	0.158	0.838
56	11.3	13	2.66E-04	F17	4.12	2.59E-05	F01	3.19	−9.79	F02	−2.32	0.786	0.606	0.181
57	22.6	10	0.0475	F22	3.15	−8.38E-06	F18	−13.1				0.964	0.0198	0.940
58	−6.61	6	1.71E-05	F01	2.27	8.19E-06	F02	4.50				0.888	0.201	0.160
59	28.0	6	−6.08	F08	−11.9	−3.12E-06	F18	−3.55				0.980	0.0346	0.956
60	13.3	10	0.00264	F19	4.60	−1.32E-05	F18	−6.49				0.900	0.206	0.807
61	11.46	7	2.23E-03	F19	5.12	−7.37E-04	F10	−4.83				0.913	0.0707	0.754
62	23.3	7	−0.0835	F22	−6.61	−0.0226	F11	−4.28				0.932	0.0123	0.270
63	5.01	13	1.66	F15	261	−2.58E-07	F04	−2.24	−1.61E-06	F18	−4.07	0.779	0.0151	0.300

[a]The numeration of ligands corresponds to Table 1.

[b]Number of data points in the set.

[c]$R^2 = 0.809$ was obtained using five descriptors (2.78 − 7.43E-07 × F18 + 8.43E-07 × F02 − 1.77E-07 × F04 + 3.60E-03 × F23 − 1.47E-06 × F01).

Table 6. The QSPR models ($a_0 + a_1d_1 + a_2d_2 + a_3d_3 + a_4d_4$) on complex stability constants for lanthanides

Metal	a_0	n[a]	a_1	d_1	*t*-test	a_2	d_2	*t*-test	a_3	d_3	*t*-test	a_4	d_4	*t*-test	R^2	s^2	R^2_{cv}
La	−6.28	76	0.00159	G01	10.9	133	H02	7.22	5.90	P02	4.74	1.26	E02	3.07	0.846	4.10	0.825
Ce	11.0	53	0.00262	G01	14.8	40.0	G02	3.80	175	H04	4.83	−5.36	T04	−5.64	0.889	2.65	0.863
Pr	8.16	58	0.101	T05	13.5	45.1	G02	5.00	90.9	P03	6.68	−3.49	B02	−3.29	0.910	2.80	0.893
Nd	− 1.82	74	0.194	G03	8.63	16.3	H03	10.5	8.47	P02	6.68	−0.909	B03	− 3.18	0.879	3.66	0.857
Sm	15.38	70	0.00157	G01	9.22	−4.27	B04	−3.07	131	H02	6.38	3.99	P02	3.27	0.863	4.43	0.843
Eu	−4.65	57	0.00210	G01	10.6	18.9	H01	3.53	5.19	P01	3.58	1.97	E02	3.98	0.897	4.03	0.878
Gd	−9.51	70	0.242	G03	9.98	1.17	E05	2.45	8.40	P02	5.96	394	H05	8.12	0.864	4.73	0.841
Tb	−6.59	58	90.1	H06	7.89	3.79	T02	7.98	3.88	P01	2.58	1.73	E05	3.28	0.873	4.27	0.846
Dy	−0.479	63	0.208	G03	7.77	17.2	H03	9.44	9.68	P02	6.46	−1.33	B03	−3.57	0.881	4.30	0.855
Ho	−28.4	57	5.91	T01	14.3	2.16	E05	3.93	11.8	T03	6.91	−458	E04	−3.48	0.897	3.75	0.880
Er	32.5	63	0.203	G03	8.35	17.4	H03	9.43	10.3	P01	6.76	−10.8	B01	−4.29	0.883	4.05	0.859
Tm	−35.6	45	6.05	T01	11.46	225	H02	8.35	−452	E03	−2.28	1.85	B01	2.86	0.910	3.91	0.888
Yb	23.9	59	4.80	T02	6.77	2.74	E01	6.05	1191	P03	7.46	−699	E03	−4.01	0.880	4.99	0.860
Lu	0.0203	58	4.24	T02	7.94	158	H02	4.80	1.52	B05	4.78	−1.46	B03	−2.93	0.860	4.97	0.835

[a]Number of data points in the set.

Table 7. Descriptors used in the QSPR models for lanthanides

	Descriptor name
	Bonding interactions
B01	Max coulombic interaction for bond H–C
B02	Min coulombic interaction for bond H–C
B03	Max coulombic interaction for bond C–C
B04	Min coulombic interaction for bond C–C
B05	Number of double bonds
	Partial surface areas
P01	Square root of charged surface area (MOPAC PC) for atom C
P02	Square root of charged surface area for atom C
P03	Square root of partial surface area for atom O
	Geometrical/constitutional
G01	Gravitation index (all atoms' pairs)
G02	Relative number of N atoms
G03	Shadow plane YZ
	Topological
T01	Average complementary information content (order 1)
T02	Average complementary information content (order 2)
T03	Average information content (order 0)
T04	Average information content (order 1)
T05	Complementary information content (order 2)
	Electronic properties
E01	HOMO-1 energy
E02	LUMO energy
E03	Max 1-electron react. index for atom O
E04	Min 1-electron react. index for atom O
E05	Tot hybridization comp. of the molecular dipole
	Hydrogen bonding
H01	HA dependent HDSA-1/TMSA (Zefirov PC)
H02	HA dependent HDSA-2/TMSA (Zefirov PC)
H03	HACA-2/SQRT(TMSA) (MOPAC PC)
H04	H-donors FCPSA (version 2)
H05	HACA-2/TMSA (MOPAC PC)
H06	HA dependent HDCA-2/SQRT(TMSA) (Zefirov PC)

surface areas 10 times, electronic properties 9 times, descriptors describing the topology 8 times, and bonding interaction descriptors 8 times.

This distribution of molecular descriptors in QSPR models indicates that the bidentate complex formation with the lanthanide ions is predominantly determined by the hydrogen-bonding related properties, geometrical and even topological structure of the ligands. The descriptors reflecting the charge distribution in the ligands and the related electrostatic interactions have smaller contributions.

In the case of the correlations with the lanthanide (metal) descriptors, the most important contribution is given by the successive ionization potentials of the metals. Those descriptors appear altogether 42 times, of which 18 cases involve the fourth ionization potential of the metal, i.e. the ionization potential of the Ln^{3+} ion. Another group of the descriptors of substantial importance includes the heats of vaporization (26 times) and fusion (8 times) of the metals. In principle, these descriptors (physical properties) depend on the London forces between the metal atoms and may thus reflect similar non-covalent interactions in the complexes.

The descriptors in each model are given in Tables 5 and 6 in order of the (absolute) *t*-test values. In this way, the most significant descriptors for each model are in the d1 column (Tables 5 and 6). If two or several metals or organic ligands have the same most significant descriptors, it follows the complex stability for those metals or organic ligands should depend predominantly on the same chemical parameter or effect.

Notably, the overall fitness of the QSPR models with metals as variables is excellent (Fig. 1). Thus, the prediction of $\log K_1$ in cases when the QSPR

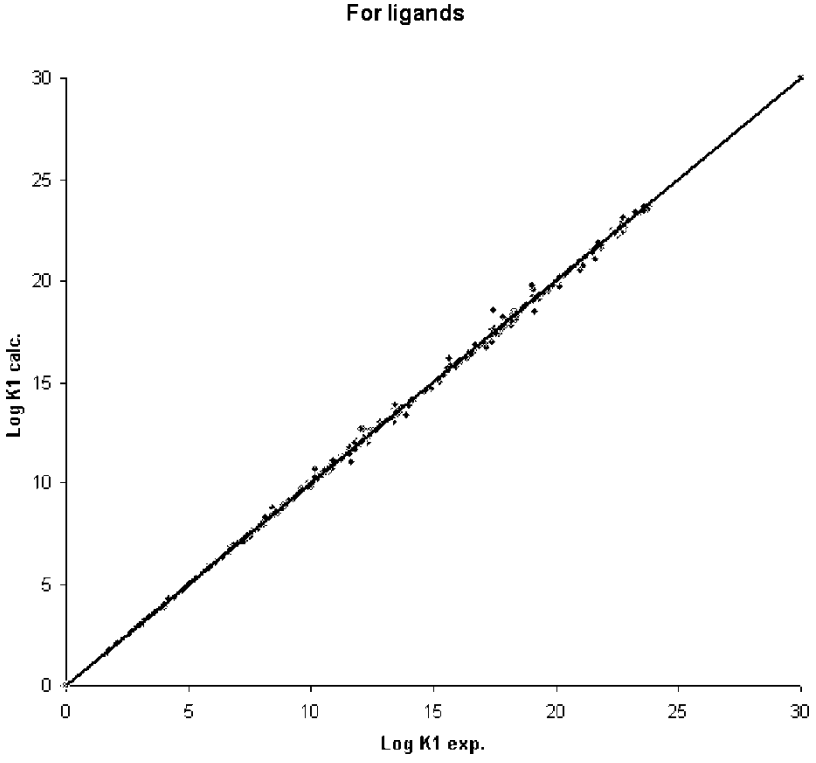

Figure 1. Correlation between the experimental and predicted data from QSPR models for single ligands (metals variable). $R^2 = 0.999$.

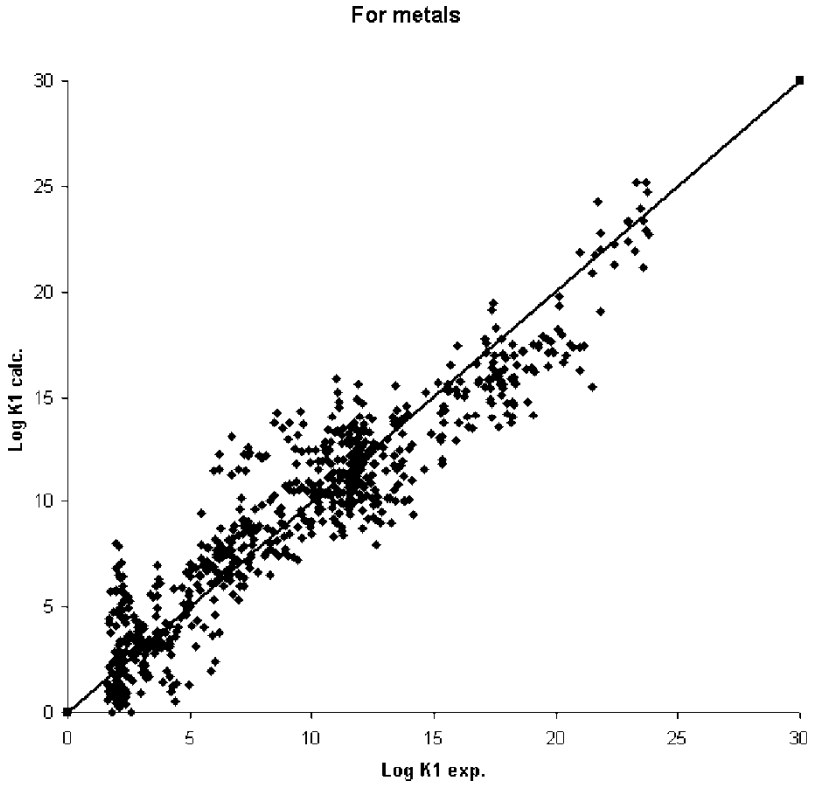

Figure 2. Correlation between the experimental and predicted data from QSPR models for single metals (ligands variable). $R^2 = 0.881$.

equation is known for a given organic ligand would be very reliable. On the other hand, the predictions from the QSPR models with ligands as variables are less precise (Fig. 2). This is, however, not unexpected bearing in mind large structural variability of the organic ligands used.

A significant correlation was found between the predictions of unknown $\log K_1$ values, proceeding from the QSPR equations for the ligands and for the metals, respectively ($R^2 = 0.6$, Fig. 3).

CONCLUSIONS

We have demonstrated that the theoretical molecular descriptors can been successfully applied in the development of predictive QSPR models for the stability constants of lanthanide (III)–organic complexes. These constants are also well correlated with various physical properties of lanthanide metals used as the descriptors characterizing the metal ions in the series of

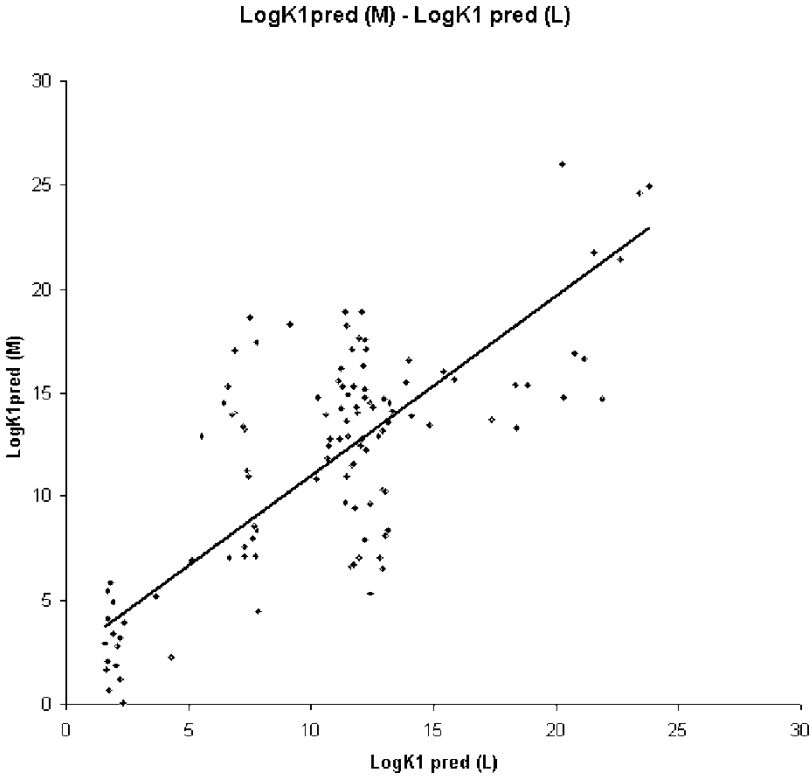

Figure 3. Correlation between the predicted data for unknown complexes from the QSPR models for metals and ligands as variable, respectively. $R^2 = 0.588$.

data for a constant organic ligand. A satisfactory correlation was found between the stability constants for previously unmeasured complexes predicted from the QSPR equations for a constant ligand and a constant metal ion, respectively.

REFERENCES

1. Furphy, B.M., Harrowfield, J.M., Kepert, D.L. et al. (1987) Bimetallic lanthanide complexes of the calixarenes: europium(III) and *t*-butylcalix[8]arene. *Inorg. Chem.*, 26: 4231–4236.
2. Howell, R.C., Spence, K.V.N., Kahwa, I.A. et al. (1996) The preparation and crystal and molecular structures of new luminescent Schiff's base complexes featuring coupled lanthanide (III) cations. *J. Chem. Soc. Dalton Trans.*, 961–968.
3. Howell, R.C., Spence, K.V.N., Kahwa, I.A., and Williams, D.J. (1998) Structure and luminescence of the neutral dinuclear lanthanide (III) complexes

[{Ln(api)}$_2$] {H_3 API = 2-(2-hydroxyphenyl)-1,3-bis[4-(2-hydroxyphenyl)-3-azabut-3-enyl]-1,3-imidazolidine}. *J. Chem. Soc. Dalton Trans.*, 2727–2733.

4. Latva, M., Mäkinen, P., Kulmala, S., and Haapakka, K. (1996) Self assembled europium(III)–lanthanide(III) chelates of 2,6-bis[*N*,*N*-bis(carboxymethyl-4-benzoylphenol)] and their radiative $^5D_0-^7F_j$ transitions of Eu^{3+}. *J. Chem. Soc. Faraday Trans.*, 92: 3321–3326.
5. Liu, S., Gelmini, L., Rettig, S.J. et al. (1992) Synthesis and characterisation of lanthanide [Ln(L)]$_2$ complexes of N_4O_3 amine phenol ligands with phenolate oxygen bridges: evidence for very weak magnetic exchange between Ln–Ln ions. *J. Am. Chem. Soc.*, 114: 6081–6087.
6. Wang, Z., Reibenspies, J., and Martell, A.E. (1997) Design, syntheses, X-ray structural characterisation of new dinuclear macrocyclic ligands and a novel phenolate-bridged dilanthanum(III) complex. *Inorg. Chem.*, 36: 629–636.
7. Aime, S., Botta, M., Fasano, M., and Terreno, E. (1998) Lanthanide(III) chelates for NMR biomedical applications. *Chem. Soc. Rev.*, 27: 19–30.
8. Lauffer, R.F. (1987) Paramagnetic metal complexes as water proton relaxation agents for NMR imaging theory and design. *Chem. Rev.*, 87: 901–927.
9. Matthews, K.D., Bailey-Folkes, S.A., and Kahwa, I.A., et al. (1992) Luminescence decay dynamics and CP MAS C-13 NMR characteristics of dinuclear complexes exhibiting couples lanthanide(III) cation pairs. *J. Phys. Chem.*, 96: 7021–7027.
10. Matthews, K.D., Fairman, R.A., Johnson, A. et al. (1993) The preparation and luminescence decay dynamics of coupled heterolanthanide(III) cations in dinuclear Schiff-base complexes. *J. Chem. Soc., Dalton Trans.*, : 1719–1923.
11. Bianchi, A., Calabi, L., Corana, F. et al. (2000) Thermodynamic and structural properties of Gd(III) complexes with polyamino-polycarboxylic ligands: basic compounds for the development of MRI contrast agents. *Coord. Chem. Rev.*, 204: 309–393.
12. Hirokawa, T. and Kiso, Y. (1984) Complex-forming Equilibria in Isotachophoresis. VI. Simulation of Isotachophoretic Equilibria of lanthanoids and Determination of Mobilities and Stability Constants of Acetate and $\propto$ -Hydroxyisobutyrate complexes. *J. Chromatogr.*, 312: 11–29.
13. Dewar, M.J.S., Zoebisch, E.G., Healy, E.F. et al. (1985) AM1: A new General Purpose Quantum Mechanical Model. *J. Am. Chem. Soc.*, 107: 3902–3909.
14. Stewart, J.J.P. (1990) *MOPAC Manual 6.0*; Seiler F. J. Research Laboratory QCE No 455.
15. Katritzky, A.R., Lobanov, V.S., and Karelson, M. (1994a) *CODESSA Reference Manual Version 2.0*; Gainesville.
16. Katritzky, A.R., Lobanov, V.S., and Karelson, M. (1995) QSPR: Correlation and Quantitative Prediction of Chemical and Physical Properties from Structure. *Chem. Soc Rev*, 279–287.
17. Katritzky, A.R., Maran, U., Karelson, M., and Lobanov, V.S. (1997) Prediction of melting points for the substituted benzenes: A QSPR Approach. *J. Chem. Inf. Comput. Sci*, 37: 913–919.
18. Huibers, P.D., Lobanov, V.S., and Katritzky, A.R. (1996) Prediction of critical micelle concentration using a quantitative structure-property relationship approach. 1. Nonionic Surfactants. *Langmuir*, 12: 1462–1470.
19. Huibers, P.D., Lobanov, V.S., Katritzky, A.R. et al. (1997) Prediction of critical micelle concentration using a quantitative structure-property relationship approach 2. Anionic Surfactants. *J. Colloid Interface Sci*, 187: 113–120.

20. Katritzky, A.R., Mu, L., and Karelson, M. (1996a) A QSPR study of the solubility of gases and vapors in water. *J. Chem. Inf. Comput. Sci.*, 36: 1162–1168.
21. Katritzky, A.R., Rachwal, P., Law, K.W., et al. (1996b) Prediction of polymer glass transition temperatures using a general quantitative structure-property relationship treatment. *J. Chem. Inf. Comput, Sci.*, 36: 879–884.
22. Katritzky, A.R., Tamm, T., and Wang, Y. (1999) QSPR treatment of solvent scales. *J. Chem. Inf. Comput, Sci.*, 39: 684–691.